Broadband and Multi-Color Large Format Infrared Focal Plane Arrays for Static Imaging Interferometers

S. D. Gunapala, S. V. Bandara, J. K. Liu, S. B. Rafol, J. M. Mumolo, F. M. Reininger, J. M. Fastenau, and A. K. Liu*

Jet Propulsion Laboratory, California Institute of Technology
4800, Oak Grove Drive, Pasadena, CA 91109
* IQE Inc., 119 Technology Drive, Bethlehem, PA 18015

ABSTRACT

A 10-16 μm cutoff large format broadband quantum well infrared photodetector (QWIP) focal plane array (FPA) has been demonstrated. The size of the FPA is 640x512 and its pixel pitch is 25 microns. The highest operating temperature of the FPA is 45K, and it was determined by the charge storage capacity and the other features of the particular readout multiplexer used in this demonstration. Excellent imagery, with a noise equivalent differential temperature (NEΔT) of 55 mK has been achieved. In this presentation, we will discuss the development of this large format broadband infrared FPA based on a GaAs/AlGaAs materials system and its performance in quantum efficiency, NEΔT, uniformity, and operability.

Keywords: Broadband, Intersubband Transitions, Infrared (IR), Long-wavelength Infrared (LWIR), Very Long-wavelength (VLWIR), Gallium Arsenide (GaAs), Quantum Well Infrared Photodetector (QWIP), Focal Plane Arrays, Noise Equivalent Temperature Difference (NEΔT), Infrared Imaging

1. INTRODUCTION

In recent years, quantum well infrared photodetectors (QWIPs) have shown very good imaging performance at high-background conditions using large area 256x256 and 640x512 highly uniform focal plane arrays (FPAs) [1-4]. Fabricated entirely from large bandgap materials which are easy to grow and process, it is now possible to obtain large uniform FPAs of QWIPs tuned to detect light at wavelengths from 6 to 25 μm in the GaAs/Al_xGa_{1-x} As material system [5]. Currently, there is a tremendous interest in long-wavelength QWIPs due to infrared (IR) imaging systems that require large format long-wavelength infrared (LWIR) FPAs for myriad applications, including night vision, navigation, flight control, early warning systems, Earth observing systems, astronomy, etc. Unlike the responsivity spectrums of intrinsic infrared detectors, the responsivity spectrums of QWIPs are much narrower and sharper due to their resonance intersubband absorption [6,7]. However, many Earth observing instrument require FPAs with broadband photoresponse. As we have demonstrated earlier, a broadband sensitive QWIP device structure can be designed by repeating a unit of several quantum wells with slightly different parameters such as well width and barrier height.

2. BROADBAND QWIP

Broadband QWIP device structure is designed by repeating a unit of several quantum wells with slightly different parameters such as well width and barrier height [8]. The positions of ground and excited states of the quantum well are determined by the quantum well width (L_w) and the barrier height, i.e. the Al mole fraction (x) of the barrier [6,7]. Since each single set of parameters for a bound-to-quasibound quantum well [9] corresponds to a spectral band pass of about 1.5 μm, three different sets of values are sufficient to cover a 10-16 μm spectral region. As shown in Fig 1, the MQW structure consists of many periods of these three-quantum-well units separated by thick barriers. The device structure reported here involved 33 repeated layers of GaAs three-quantum-well units separated by $L_B \sim 575$ Å thick $Al_xGa_{1-x}As$ barriers (See Fig 1). The well thickness of the quantum wells (see Fig. 1) of three-quantum-well units are designed to respond at peak wavelengths around 13, 14, and 15μm respectively. These wells are separated by $L_u \sim 75$ Å thick $Al_xGa_{1-x}As$ barriers. The Al mole fraction (x) of barriers throughout the structure was chosen such that the $\lambda_p = 13$ μm

quantum well operates under bound-to-quasibound conditions [9]. The excited state energy level broadening has been further enhanced due to the overlap of the wavefunctions associated with excited states of quantum wells separated by thin barriers. Energy band calculations based on a two band model show excited state energy levels spreading about 28 meV.

The sample was grown on a semi-insulating 3-inch GaAs substrate by molecular beam epitaxy. It consists of the device structure described above sandwiched between top and bottom contact layers. Transport carriers (electrons) were provided by doping all GaAs wells and contact layers with Si. In order to measure dark current-temperature curve, spectral responsivity (see figure 2-4) and noise, 200 μm diameter mesas were fabricated using wet chemical etching and Au/Ge ohmic contacts were evaporated onto the top and bottom contact layers.

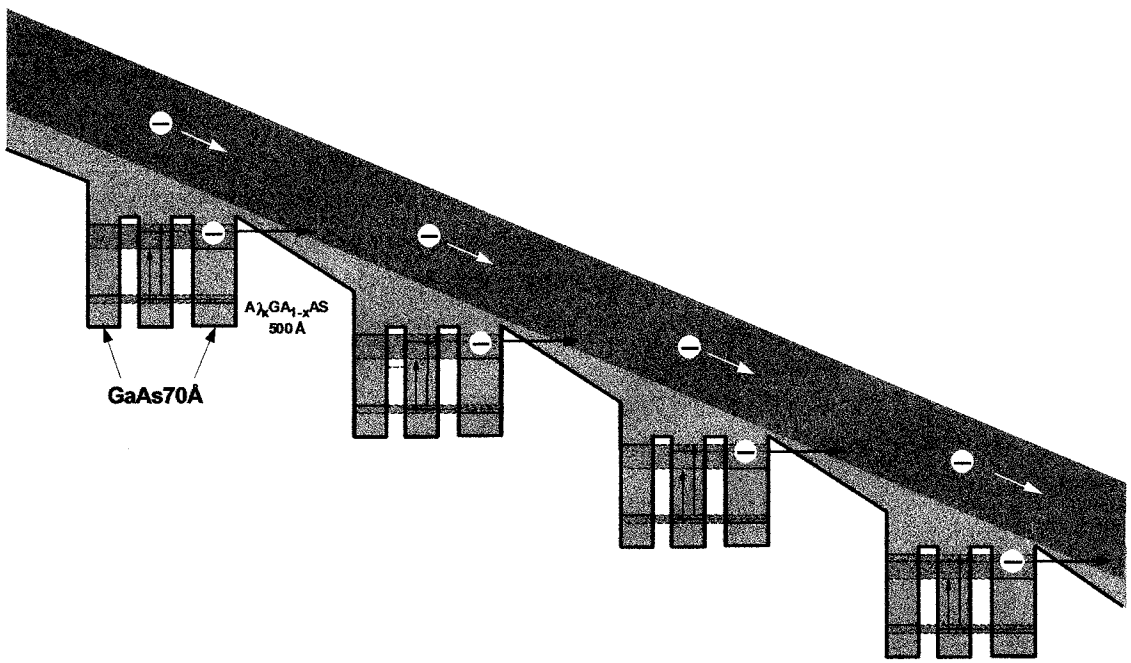

Fig. 1. Broad-band MQW structure is designed by repeating a unit of several quantum wells with slightly different parameters such as well width and barrier height. The excited state energy levels broadened due to overlap of the wavefunctions associated with excited states of quantum wells separated by thin barriers.

The responsivity spectra of these detectors were measured using a 1000 K blackbody source and a grating monochromator. The detectors were back illuminated through a 45° polished facet to obtain normalized responsivity spectra at different bias voltages. Then the absolute spectral responsivities were obtained by measuring total photocurrent from a calibrated black-body source. In Fig. 3, responsivity curve at V_B = -2.5 V bias voltage shows broadening of the spectral response up to $\Delta\lambda \sim 5.5$ μm, i.e. the full width at half maximum from 10.5 - 16μm. This broadening $\Delta\lambda/\lambda_p \sim 42$ % is about a 400 % increase compared to a typical bound-to-quasibound QWIP [8].

Unlike narrow-band QWIPs, these detectors show spectral peak shifts from λ = 11.5 μm to λ = 15.1 μm as negative bias voltage increased from V_B = -1 V to V_B = -5 V and similar behavior (λ = 11.5 μm to λ = 14.7 μm for V_B = +1 V to V_B = +5 V) was observed under positive bias voltages as well. This suggests that there is no substantial carrier depletion due to the applied electric field within the three-quantum-units because the direction of peak shift remains the same under both positive and negative biases [8]. The responsivity of the detector peaks at 13.5 μm and the peak responsivity (R_p) of the detector is 250 mA/W at bias V_B = -2.5 V. The bias dependent peak responsivity of the detector is shown in Fig. 4. The measured absolute peak responsivity of the detector is small, up to about V_B = -0.5 V. Beyond that it increases

nearly linearly with bias reaching R_P = 580 mA/W at V_B = -3.5 V. This type of behavior of responsivity versus bias is typical for a bound-to-quasibound QWIP. The peak quantum efficiency was 11% at bias V_B = -2.5 V for a 45° double pass. The lower quantum efficiency is due to the lower well doping density ($2x10^{17}$ cm^{-3}) as it is necessary to suppress the dark current at the highest possible operating temperature. A peak quantum efficiency as high as 25% has already been achieved with regular well doping density (i.e., $1x10^{18}$ cm^{-3}). Due to lower readout multiplexer well depth (i.e., $11x10^6$ electrons) a lower dark current is mandatory to achieve a higher operating temperature. In this case, the highest operating temperature of 45 K was determined by the well depth of the readout multiplexer.

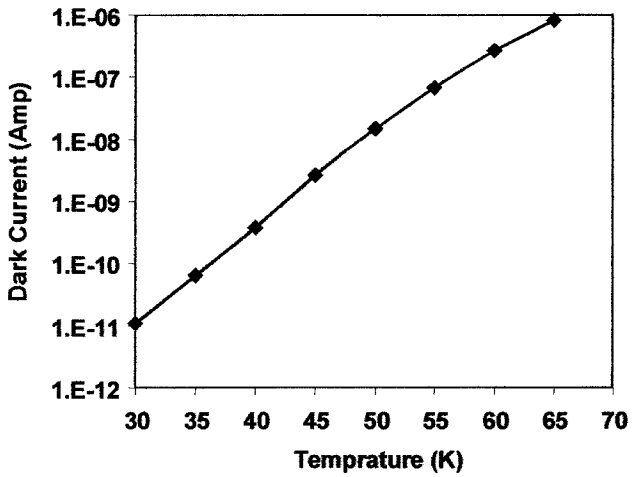

Fig. 2. Dark current-temperature curve of 10-15.4 μm broadband QWIP at bias V_B = -2.5V. Data were taken with a 200 μm diameter test structure and normalized to 25x25 μm^2 pixel.

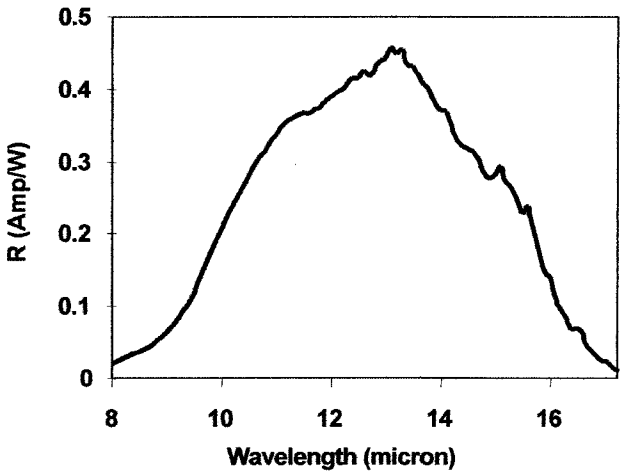

Fig. 3. Responsivity spectrum of a broadband QWIP test structure at temperature T = 55 K. The spectral response peak is at 13.5 μm and the long wavelength cutoff is at 15.4 μm.

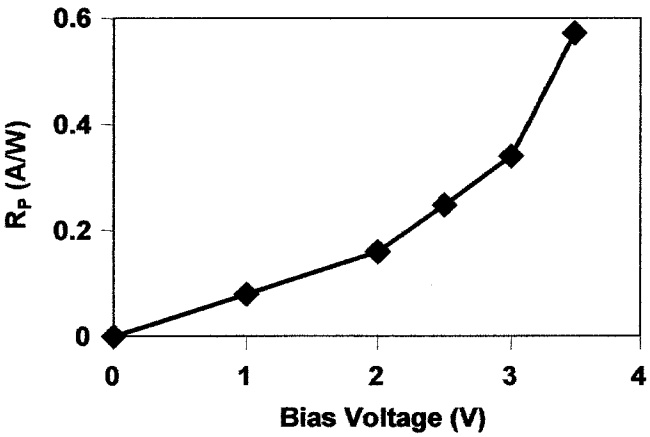

Fig. 4. Peak responsivity as a function of bias voltage at temperature T = 55 K.

The dark current noise i_n of the device was measured using a spectrum analyzer at T = 55 K as a function of bias voltage. The noise gain g_n can now be obtained using the g-r noise calculated based on standard noise expression: $i_n = \sqrt{4eI_d g_n \Delta B}$ where I_d is the dark current and ΔB is the band width. Using experimental measurements of noise and responsivity, one can now calculate specific detectivity D^* form $D^* = R\sqrt{A\Delta f} / i_n$, where A is area of the detector. Calculated D* value for the present device (λ = 15.4 μm) at, T = 55 K, and V_B = 2.5 V is 3 x 10^{10} cm $\sqrt{Hz}$ /W. Even with broader response, this D^* is comparable to previously reported D^* of QWIPs with narrow spectral response. Figures 5 and 6 show the detectivity D* and the noise equivalent temperature difference (NEΔT) as a function of the operating temperature of the device.

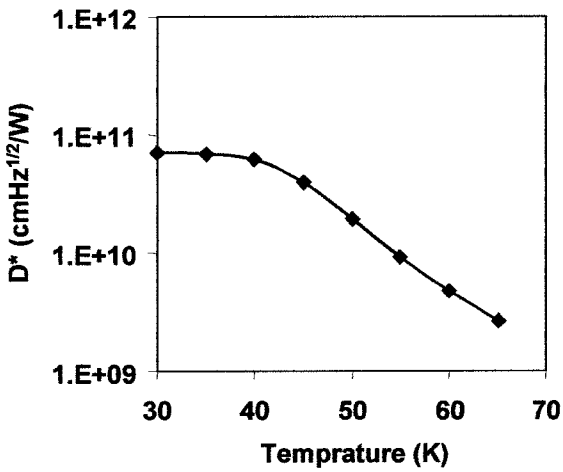

Fig. 5. Detectivity as a function of temperatures at bias voltage V_B = -2.5V.

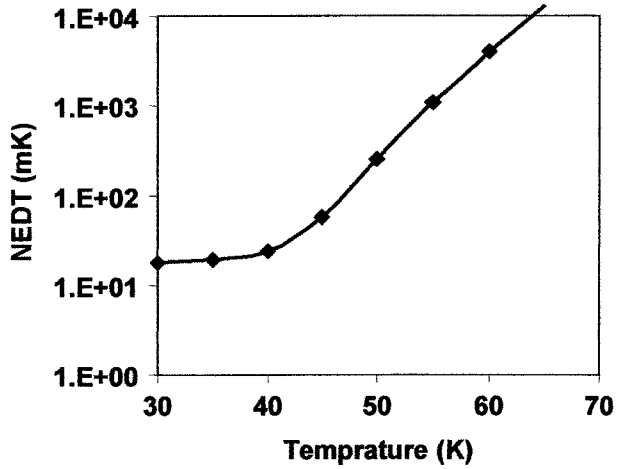

Fig. 6. Noise equivalent temperature difference as a function of temperatures at bias voltage V_B = -2.5V.

3. 640x512 BROADBAND QWIP FOCAL PLANE ARRAY

It is well known that QWIPs do not absorb radiation incident normal to the surface unless the IR radiation have an electric field component normal to the layers of superlattice (growth direction) [6]. As we have discussed before [6,7] many more passes of IR light inside the detector structure can be obtained by incorporating a randomly roughened reflecting surface on top of the detectors which also removes the light coupling limitations and makes two dimensional QWIP imaging arrays feasible. This random structure was fabricated on the detectors by using standard photolithography and CCl_2F_2 selective dry etching. The advantage of the photolithographic process over a completely random process is the ability to accurately control the feature size and preserve the pixel to pixel uniformity which is a prerequisite for high sensitivity imaging FPAs.

After the random reflector array was defined by the lithography and dry etching, the photoconductive QWIPs of the 640x512 FPAs were fabricated by dry etching through the photosensitive GaAs/$Al_xGa_{1-x}As$ multi-quantum well layers into the 0.5 μm thick doped GaAs bottom contact layer. The pitch of the FPA is 25 μm and the actual pixel size is 23x23 μm^2. The random reflectors on top of the detectors were then covered with Au/Ge and Au for Ohmic contact and reflection. Figure 7 shows twelve processed QWIP FPAs on a 3-inch GaAs wafer. Indium bumps were then evaporated on top of the detectors for Si readout circuit (ROC) hybridization. A single QWIP FPA was chosen and hybridized (via indium bump-bonding process) to a 640x512 CMOS multiplexer (Indigo Systems 9803) and biased at V_B = -2.5 V (see figure 8). At temperatures below 48 K, the signal to noise ratio of the system is limited by array non-uniformity, multiplexer readout noise, and photo current (photon flux) noise (see Figure 9). At temperatures above 48 K, temporal noise due to the QWIP's higher dark current becomes the limitation. As mentioned earlier this higher dark current is due to thermionic emission and thus causes the charge storage capacitors of the readout circuitry to saturate. Since the QWIP is a high impedance device, it should yield a very high charge injection coupling efficiency into the integration capacitor of the multiplexer. In fact Bethea *et al.* [10] have demonstrated charge injection efficiencies approaching 90%.

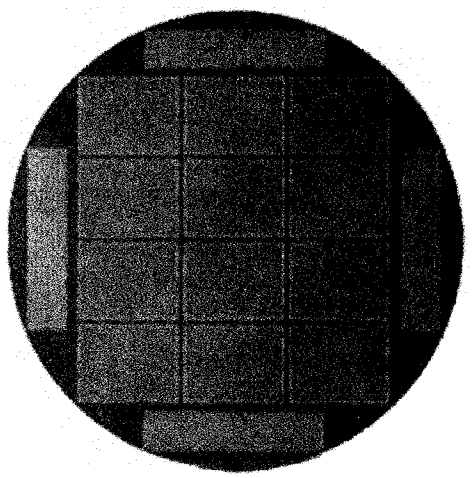

Fig. 7. Twelve 640x512 QWIP focal plane arrays on a 3 in. GaAs wafer.

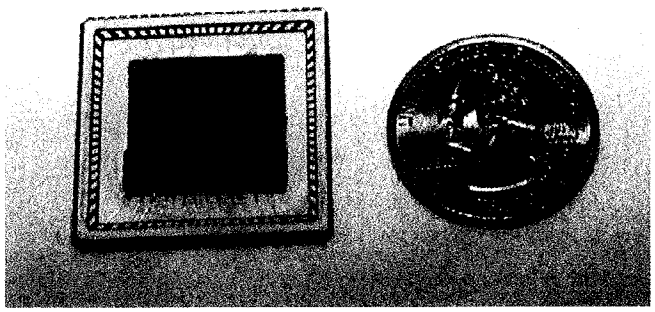

Fig. 8. A size comparison of the 640 x 512 long-wavelength QWIP FPA to a quarter.

Charge injection efficiency can be obtained from [3]

$$\eta_{inj} = \frac{g_m R_{Det}}{1+g_m R_{Det}} \left[\frac{1}{1+\frac{j\omega C_{Det} R_{Det}}{1+g_m R_{Det}}} \right] \quad (1)$$

where g_m is the transconductance of the MOSFET and is given by $g_m = eI_{Det}/kT$. The differential resistance R_{Det} of the pixels at -2 V bias is 5.4×10^{10} Ohms at T=45 K and detector capacitance C_{Det} is 1.4×10^{-14} F. The detector dark current I_{Det} = 8 pA under the same operating conditions. According to equation (1) the charge injection efficiency η_{inj}=99.5% at a frame rate of 30 Hz. The FPA was back- illuminated through the flat thinned substrate membrane (thickness ≈ 1300 Å). This thinned GaAs FPA membrane has completely eliminated the thermal mismatch between the silicon CMOS readout multiplexer and the GaAs based QWIP FPA. Basically, the thinned GaAs based QWIP FPA membrane adapts to the thermal expansion and contraction coefficients of the silicon readout multiplexer. Thus, thinning has played an extremely important role in the fabrication of large area FPA hybrids. In addition, this thinning has completely eliminated the pixel-to-pixel optical cross-talk of the FPA. This initial array gave very good images with 99.9% of the pixels working, demonstrating the high yield of GaAs technology. The operability was defined as the percentage of pixels having noise equivalent differential temperature less than 100 mK at 300 K background with f/2 optics and in this case operability happens to be equal to the pixel yield.

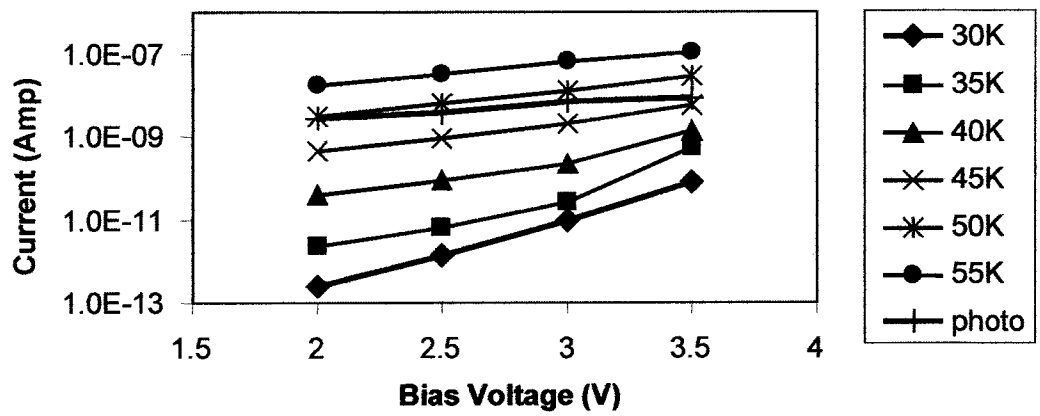

Fig. 9. Dark current and the photo current of 10-15.4 μm broadband QWIP as a function of bias voltage.

We have used the following equation to calculate the NEΔT of the FPA.

$$NE\Delta T = \frac{\sqrt{AB}}{D_B^*(dP_B/dT)\sin^2(\theta/2)} \quad (2)$$

where D_B^* is the blackbody detectivity, dP_B/dT is the derivative of the integrated blackbody power with respect to temperature, and θ is the field of view angle [i.e., $\sin^2(\theta/2) = (4f^2+1)^{-1}$, where f is the f number of the optical system]. The background temperature T_B = 300 K, the area of the pixel A = (23 μm)^2, the f number of the optical system is 2, and the frame rate is 30 Hz. Figure 10 shows the experimentally measured NEΔT histogram of the FPA at an operating

temperature of T = 35 K, bias V_B = -2.5 V at 300 K background with f/2 optics and the mean value is 55 mK. This agrees reasonably well with our estimated value of 25 mK based on test structure data. The read noise of the multiplexer is 500 electrons. The factor of two shortfall of NEΔT is mostly attributed to decrease in bias voltage across the detectors during charge accumulation (common in many direct injection type readout multiplexers) and read noise of the readout multiplexer. The experimentally measured peak quantum efficiency of the FPA was 9.5% which agrees well with the 11% quantum efficiency estimated from the single element detector data.

4. IMAGERY WITH BROADBAND ARRAY

A 640X512 QWIP FPA hybrid was mounted onto a 84-pin lead-less chip carrier and installed into a laboratory dewar which is cooled by liquid neon to demonstrate a LWIR imaging camera (FPA was cooled to 35K). The other element of the camera is a 100 mm focal length AR coated germanium lens, which gives a 9.2°x6.9° field of view. It is designed to be transparent in the 8-12 μm wavelength range (which is not fully compatible with the 10-15 micron broadband QWIP array). SEIR image processing station was used to obtain clock signals for readout multiplexer and to perform digital data acquisition and non-uniformity corrections. The digital data acquisition resolution of the camera is 14-bits, which determines the instantaneous dynamic range of the camera (i.e., 16,384), however, the dynamic range of QWIP is 85 Decibels.

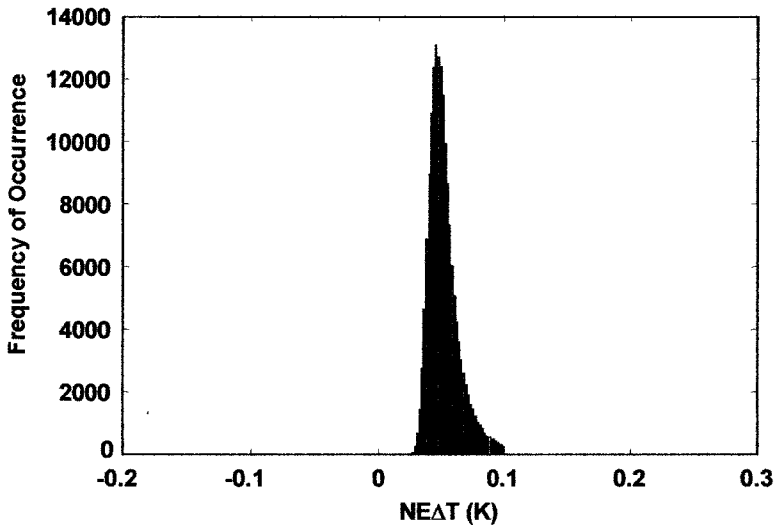

Fig. 10. Noise equivalent temperature difference (NEΔT) histogram of the 327,680 pixels of the 640 x 512 array showing a high uniformity of the FPA. The uncorrected non-uniformity (= standard deviation/mean) of this unoptimized FPA is only 6.3% including 1% non-uniformity of ROC and 1.4% non-uniformity due to the cold-stop not being able to give the same field of view to all the pixels in the FPA.

The measured mean NEΔT of the QWIP camera is 55 mK at an operating temperature of T = 35 K and bias V_B = -2.5 V at 300 K background with f/2 optics. This is in good agreement with expected focal plane array sensitivity due to the practical limitations on charge handling capacity of the multiplexer, read noise, bias voltage and operating temperature. The uncorrected NEΔT non-uniformity (which includes a 1% non-uniformity of the ROC and a 1.4% non-uniformity due to the cold-stop in front of the FPA not yielding the same field of view to all the pixels) of the 327,680 pixels of the 640x512 FPA is about 6.3% (= sigma/ mean). The non-uniformity after two-point (17° and 27° Celsius) correction improves to an impressive 0.1%. As mentioned earlier, this high yield is due to the excellent GaAs growth uniformity and the mature GaAs processing technology.

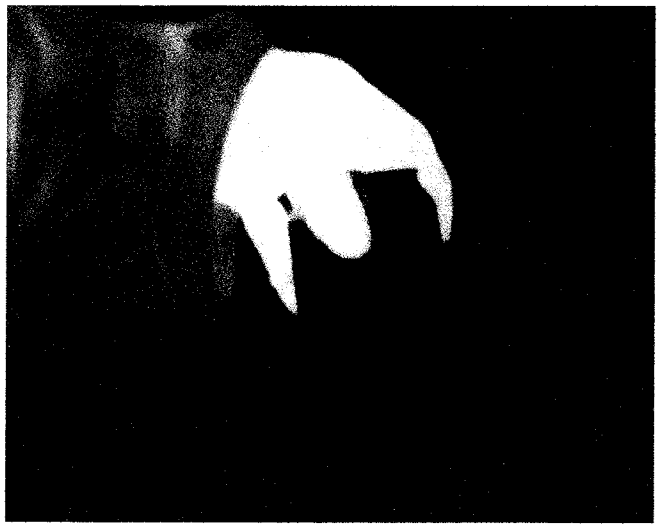

Fig. 11. This picture shows a frame of video image taken with this 10-15.4 mm 640x512 broadband QWIP imager. This image shows the liquide level of the soda can and some finger prints on the can.

Video images were taken at a frame rate of 15 Hz at temperatures as high as T = 35 K using a ROC capacitor having a charge capacity of $11x10^6$ electrons (the maximum number of photoelectrons and dark electrons that can be counted in the integration time of each detector pixel). Figure 11 shows a frame of video image taken with this 10-15.4 mm 640x512 broadband QWIP imager. These high resolution images comparable to standard TV, demonstrate the high operability (i.e., 99.9%) and the stability (i.e., lower residual uniformity and 1/f noise) of the 640 x 512 long-wavelength QWIP staring array camera. It should be noted that these initial unoptimized FPA results are far from optimum. The light coupling gratings were not optimized (as described earlier) for maximum light coupling efficiency, no anti-reflection coatings were used on the backside of the FPA.

5 BROADBAND QWIPs FOR THERMAL INFRARED IMAGING SPECTROMETERS

Until recently, QWIP detectors have been available only over narrow bands (typically 1.0 - 2.0 μm wide) in the 6 - 20 μm spectral range. Bandara *et al.* [8] have developed a broadband test detector that will cover the 10 -16 μm band and FPAs of these detectors are mated to a 640x512 multiplexer (see Fig. 8). This detector has been developed specifically for thermal infrared imaging spectrometers—anticipating a possible need for Mars exploration. This program required a thermal infrared imaging spectrometer with minimum power, mass, and volume. One attractive instrument concept involved a Spatially Modulated Infrared Spectrometer (SMIS) to cover the LWIR and VLWIR spectral ranges. This instrument does not contain any moving mirrors because it uses the spatially modulated Fourier Transform spectroscopy technique. Another advantage of this concept is that it has a substantially higher signal flux because all of the photons entering the pupil are used. The high spectral resolution version of this instrument requires larger format FPAs (at least 640x512) with high pixel to pixel uniformity. The lack of large format, uniform LWIR and VLWIR FPA technology has prevented the development of such highly sensitive and robust thermal infrared spectrometers. That has changed recently due to demonstration of highly uniform, large format QWIP FPAs with lower 1/f noise, at a lower cost than any other LWIR detector. In addition, the use of external filters can be avoided because QWIP can be designed to have sharp spectral cut-offs at required wavelengths. Francis Reininger, at JPL, has demonstrated this concept by building a prototype laboratory instrument working with a 8-9 μm QWIP 640x486 FPA. The unique characteristic of this instrument (besides being small and efficient) is that it has one instrument line shape for all spectral colors and spatial field positions. By using broad-band QWIP arrays with wavelengths out to 16 μm, the next version of this instrument could become the first compact, high resolution thermal infrared, hyper-spectral imager with a single spectral line shape and zero spectral smile. Such an instrument is in strong demand by scientists studying Earth and planetary science.

ACKNOWLEDGEMENT

The research described here was performed by the Center for Space Microelectronics Technology, Jet Propulsion Laboratory, California Institute of Technology, and was sponsored by the National Aeronautics and Space Administration, breakthrough sensor & instrument component technology thrust area of the cross enterprise technology development program.

REFERENCES

1. Sarath D. Gunapala, Jin S. Park, Gabby Sarusi, True-Lon. Lin, John K. Liu, Paul D. Maker, Richard E. Muller, Craig A. Shott, and Ted Hoelter, IEEE Trans. Electron Devices, 44, pp. 45-50, (1997).

2. Sarath D. Gunapala, John K. Liu, Jin S. Park, Mani Sundaram, Craig A. Shott, Ted Hoelter, True-Lon Lin, S. T. Massie, Paul D. Maker, Richard E. Muller, and Gabby Sarusi", IEEE Trans. Electron Devices, **44**, pp. 51-57 (1997).

3. S. D. Gunapala, S. V. Bandara, J. K. Liu, W. Hong, M. Sundaram, P. D. Maker, R. E. Muller, R. Carralejo, and C. A. Shott, IEEE Trans. Elec. Devices **45**, 1890 (1998).

4. S. D. Gunapala, S. V. Bandara, A. Singh, J. K. Liu, S. B. Rafol, E. M. Luong, J. M. Mumolo, N. Q. Tran, J. D. Vincent, C. A. Shott, J. Long, and P. D. LeVan, **47**, pp. 963-971, (2000).

5. S. D. Gunapala, S. V. Bandara, J. K. Liu, E. M. Luong, S. B. Rafol, J. M. Mumolo, D. Z. Ting, J. J. Bock, M. E. Ressler, M. W. Werner, P. D. LeVan, R. Chehayeb, C. A. Kukkonen, M. Levy, P. LeVan, and M. A. Fauci", Sensors and Materials, **12**, pp. 327-351, (2000).

6. S. D. Gunapala and S. V. Bandara, Physics of Thin Films, edited by M. H. Francombe, and J. L. Vossen, Vol. 21, pp. 113-237, Academic Press, NY, (1995).

7. S. D. Gunapala and S. V. Bandara, Quantum Well Infrared Photodetector (QWIP) Focal Plane Arrays, *Semiconductors and Semimetals*, 62, 197-282, Academic Press. (1999).

8. S. V. Bandara, S. D. Gunapala, J. K. Liu, E. M. Luong, J. M. Mumolo, W. Hong, D. K. Sengupta, and M. J. McKelvey, Appl. Phys. Lett. **72**, 2427 (1998).

9. S. D. Gunapala, J. K. Liu, J. S. Park, T. L. Lin, and M. Sundaram "INFRARED RADIATION DETECTING DEVICE", US Patent No. 6,211,529.

10. C. G. Bethea, B. F. Levine, M. T. Asom, R. E. Leibenguth, J. W. Stayt, K. G. Glogovsky, R. A. Morgan, J. D. Blackwell, and W. J. Parrish, IEEE Trans. Electron. Devices, **40**, pp. 1957-1963, (1993).